Internal Stresses as Origin of the Anomalous Low-Temperature Specific Heat in Glasses

Walter Schirmacher
Institut für Physik, Staudinger Weg 7, Universität Mainz, D-55099 Mainz, Germany and
Center for Life Nano Science @Sapienza, Istituto Italiano di Tecnologia, 291 Viale Regina Elena, I-00161 Roma, Italy

Giancarlo Ruocco
Dipartimento di Fisica, Sapienza Università di Roma, Piazzale Aldo Moro 2, 00185 Rome, Italy and
Center for Life Nano Science @Sapienza, Istituto Italiano di Tecnologia, 291 Viale Regina Elena, I-00161 Roma, Italy

(Received 16 December 2024; revised 22 May 2025; accepted 12 August 2025; published 17 September 2025)

We apply a recently developed theory of the nonphononic vibrational density of states (DOS) in glasses to investigate the impact of local frozen-in stresses on the low-temperature specific heat. Using a completely harmonic description we show that the hybridization of the local nonphononic vibrational excitations with the waves leads to a low-frequency DOS, in excess to the Debye one, which varies linearly with frequency up to a certain crossover frequency, and then becomes constant. The actual value of the crossover depends of the ratio between the local stresses and the shear modulus. This excess DOS leads to a low-temperature specific heat with an apparent temperature exponent, which is between one and two, as observed experimentally. We discuss how these findings may be utilized for the characterization of glassy materials. We further compare our findings, which only rely on harmonic interactions, with the predictions of other theories, which invoke anharmonic interactions and tunneling for explaining the low-temperature behavior of the specific heat.

DOI: 10.1103/p95w-9wjc

The low-frequency spectral properties of glasses and the related low-temperature properties are very different from those of their crystalline counterparts. [1–3]. For example, the specific heat of glasses does not show the Debye temperature (T) law $C(T) \sim T^3$, observed in crystals, but, instead, varies approximately as $C(T) \sim T^\alpha$ with an exponent α between 1 and 2 [1–8].

A first interpretation of the very-low temperature thermal anomalies of glasses was given by Anderson *et al.* and Phillipps in 1972 [9,10]. It was conjectured that in a glass bistable structural configurations would exist, characterized by a double-well potential as a function of some configurational coordinate. Further, tunneling between adjacent potential wells was assumed to be possible, which establishes quantum-mechanical two-level systems (TLS). It was then assumed that such TLS defect centers exist with a certain concentration and with a broad (constant) distribution, $P(\Delta E)$, of energy splittings, ΔE. This TLS model leads to a specific heat varying linearly with temperature ($\alpha = 1$).

Although the tunneling model is nowadays widely accepted as explanation of the low-temperature anomalies [11], and is even called "standard tunneling model" [12], severe criticism has been expressed [13]. Indeed, in the temperature range of 1 K the thermal de-Broglie wavelength of matter waves $\lambda = h[mk_BT]^{-1/2}$ (where h and k_B are the Planck and Boltzmann constants, and m is the mass of a molecular unit) is only a few percent of an angstrom for atomic masses larger than 10, which makes the existence of quantum tunneling in this temperature regime rather improbable. It has, however, been pointed out that bistable structural rearrangements might involve rather small single-atom displacements, which would then allow for quantum tunneling [14,15].

Alternative suggestions for explaining the low-temperature thermal anomalies of glasses are based on interacting defects [13], on elastic dipoles [16], or on the soft-potential model, which relies on the assumption of anharmonic defect states [17–19]. Most of the presently existing specific heat data have been evaluated using the TLS and soft-potential models [3,20].

As mentioned, the existing explanations of the anomalous low-T behavior of the specific heat rely mainly on the presence of *anharmonic* interactions, often in the form of double-well shaped interatomic potentials. Here, we propose another possibility of explaining the low-temperature anomalies of the specific heat, which does invokes neither quantum mechanics, nor anharmonicity. We present arguments that the spectral density of harmonic vibrations (density of states, DOS) $g(\omega)$ contains a low-frequency contribution, in addition to the Debye $g(\omega) \sim \omega^2$ law which leads to a specific heat with a scaling exponent α which turns from 1 to 2 on lowering the temperature. These contributions arise from a vortex-shaped pattern of vibrations around local frozen-in stresses.

The presence of frozen-in stresses in glasses is well known to glass blowers and is widely used for industrial applications,

e.g. tailoring the surface properties of utility materials [21]. Evidence for the (unavoidable) existence of local, randomly distributed stresses in glasses has been presented in the literature from computer simulations [22–24] and from considering the microscopic derivation of continuum elasticity [25–28]. Experimentally internal stresses may be measured by indentation [29] or by x-ray diffraction [30].

In a recent study, based on an entirely harmonic analysis, the continuum limit of the Hessian (dynamical) matrix of a glass was studied [28]. It was found, that the low-frequency nonphononic (not wavelike) vibrational excitations of small computer-simulated glasses are mainly governed by the local stresses. The nonphononic character of the excitations was guaranteed by considering small enough systems, which do not allow for low-frequency waves. By combining theory with molecular-dynamics simulations, these excitations (called "type-II modes") were identified as nonirrotational, vortexlike states [28]. The spectrum of these states was shown to be related to the distribution of small stresses. Small stresses imply small forces, which occur at molecular separations, where the interparticle-interaction potential has small values of its first derivative. In numerical simulations this artificially makes the low-frequency DOS very sensitive to the smoothed cutoff (tapering). A tapering, which guarantees continuity of the first two derivatives of the potential ($m = 2$) was shown to result in a DOS scaling as $g(\omega) \sim \omega^4$, whereas a tapering with $m = \infty$ leads to $g(\omega) \sim \omega^3$. In real systems, for potentials with a minimum (like a Lennard-Jones potential) a scaling according to $g(\omega) \sim \omega^5$ emerges. These results were obtained by considering the modification of the frequency-dependent shear modulus by the nonphononic excitations in the *absence* of waves in the interesting small frequency region. [28].

In the following we turn our attention to real, macroscopic, glasses and consider the influence of such vortexlike vibrational states on the DOS, coexisting with wavelike excitations in the same frequency range. We shall show that, in addition to the modification of the shear elasticity, there exists also a direct contribution to the low-frequency DOS, which just reflects the statistics of the local stresses. As already mentioned, such small stresses arise from the minimum of the intermolecular potentials, and exhibit a flat distribution, resulting in a DOS, which depends only weakly on frequency.

In Refs. [27,28,31] it was shown that the continuum limit of the harmonic energy of a system, interacting via a pair potential $\phi(r_{ij})$, does not only involve the usual strain degrees of freedom, as considered in elasticity theory [32] and in heterogeneous-elasticity theory [33–35], but also nonirrotational, vortexlike vibrational modes, which are associated with local stresses and are coupled via these stresses to the elastic degrees of freedom.

The vorticities are defined in terms of vortexlike vibrational displacement fields $\boldsymbol{u}_\ell(\boldsymbol{r})$ centered around a local stress at $\boldsymbol{r}_\ell$ as

$$\boldsymbol{\eta}_\ell = \frac{1}{2}\nabla \times \boldsymbol{u}_\ell(\boldsymbol{r}). \tag{1}$$

The vortexlike local displacements, therefore, may be schematically expressed as

$$\boldsymbol{u}_\ell(\boldsymbol{r}) = -\tilde{\boldsymbol{r}}_\ell \times \boldsymbol{\eta}_\ell(\tilde{\boldsymbol{r}}_\ell), \tag{2}$$

with $\tilde{\boldsymbol{r}}_\ell = \boldsymbol{r} - \boldsymbol{r}_\ell$. The vorticiy fields $\boldsymbol{\eta}$ are supposed to vanish for large values of $|\tilde{\boldsymbol{r}}_\ell|$.

In a simplified description, that we are going to present here, we treat the local stresses σ_ℓ and the vorticities $\eta_\ell(\tilde{\boldsymbol{r}}_\ell, t) = |\boldsymbol{\eta}_\ell(\tilde{\boldsymbol{r}}_\ell, t)|$ as scalars. Further, we do not treat the elastic constants μ and K (shear and bulk modulus) as fluctuating quantities, as assumed in Refs. [33–35], because the focus is here on the influence of the local stresses. Consequently, in the present treatment, the longitudinal and transverse sound velocities

$$v_L^2 = \frac{1}{\rho_m}\left[K + \frac{4}{3}\mu\right], \qquad v_T^2 = \frac{1}{\rho_m}\mu \tag{3}$$

are also not considered to vary spatially. In (3) ρ_m is the mass density. Including such spatially fluctuating elastic constants makes it possible to include the description of vibrational anomalies at higher frequencies ("boson peak") [28,33,34,36]. The coupled equations of motion for the longitudinal (L) and transverse (T) elastic fields $\boldsymbol{u}_{L,T}(\boldsymbol{r}, t)$ and the vorticities $\eta_\ell(\tilde{\boldsymbol{r}}_\ell, t)$ can be written as [28]

$$\begin{aligned}
&\rho_m[\ddot{\boldsymbol{u}}_{L,T}(\boldsymbol{r}, t) - v_{L,T}^2 \nabla^2 \boldsymbol{u}_{L,T}(\boldsymbol{r}, t)] = \sum_\ell \gamma_{L,T}^\ell \sigma_\ell \nabla \eta_\ell(\tilde{\boldsymbol{r}}_\ell, t), \\
&\zeta\, \ddot{\eta}_\ell(\tilde{\boldsymbol{r}}_\ell, t) + \sigma_\ell \eta(\tilde{\boldsymbol{r}}_\ell, t) = \sum_{\alpha=L,T} \gamma_\alpha^\ell \sigma_\ell \nabla \cdot \boldsymbol{u}_{L,T}(\boldsymbol{r}, t).
\end{aligned} \tag{4}$$

Here $\gamma_{L,T}^\ell$ are coupling coefficients of the elastic strains with the local defect-induced rotational vibrations and may be considered to be a measure for the number of molecules involved in the anomalous mode with label ℓ.

ζ is an average local moment-of-inertia density

$$\zeta = \frac{1}{4}\rho_m \langle r_\perp^2 \rangle \tag{5}$$

where $\langle r_\perp^2 \rangle$ is an average distance of the excitations from the defect center.

We emphasize here, that in deriving these equations [28], the only underlying assumptions are that the glass is composed of pairwise potentials, that it is stable, and that it is structurally disordered.

The mutual coupling between the waves and the vortices causes a renormalization of the diagonal Green's functions of the vortices (label ℓ) and the waves (label $\alpha = L, T$), see Appendix A:

$$G_{\ell\ell}(\omega) = \frac{1}{-\omega^2 + \frac{1}{\zeta}\sigma_\ell + \Delta_\ell(\omega)}, \tag{6}$$

$$G_{\alpha\alpha}(k,\omega) = \frac{1}{-\omega^2 + k^2 v_\alpha^2 + \Delta_{\alpha\alpha}(k,\omega)}. \tag{7}$$

The frequency variable ω^2 is understood to include an infinitesimally small positive imaginary part. The self-energies $\Delta_{\alpha\alpha}(k,\omega)$ and $\Delta_\ell(\omega)$ describe the hybridization of the waves and the local vibrational excitations:

$$\Delta_\ell(\omega) = \frac{\sigma_\ell^2}{\rho_m \zeta} \sum_{\alpha=L,T} \left(\frac{\gamma_\alpha^\ell}{v_\alpha}\right)^2, \tag{8}$$

$$\Delta_{\alpha\alpha}(k,\omega) = \frac{k^2}{\rho_m \zeta} \sum_\ell \gamma_\alpha^{\ell 2} \sigma_\ell^2 G_{\ell\ell}^{(0)}(\omega) = \frac{k^2}{\rho_m} \Delta M_\alpha(\omega). \tag{9}$$

As pointed out in [28], the wave renormalization gives rise to a frequency dependence of effective elastic constants defined by

$$M_\alpha(\omega) = \rho_m v_\alpha^2 + \Delta M_\alpha(\omega), \tag{10}$$

so that we have

$$G_{\alpha\alpha}(k,\omega) = \frac{1}{-\omega^2 + \frac{1}{\rho_m} M_\alpha(\omega) k^2}. \tag{11}$$

The density of states is then given by

$$\begin{aligned} g(\omega) &= \frac{2}{\pi N} \omega \,\mathrm{Im} \left\{ \left\langle \sum_{\boldsymbol{k}} G_{LL}(k,\omega) \right. \right. \\ &\quad \left. \left. + 2G_{TT}(k,\omega) + G_{\ell\ell}(\omega) \right\rangle_{P(\sigma)} \right\} \\ &= g_D(\omega) + \Delta g_{\mathrm{ind}}(\omega) + \Delta g_{\mathrm{dir}}(\omega). \end{aligned} \tag{12}$$

Here $\langle \ldots \rangle_{P(\sigma)}$ indicates an average over the distribution density $P(\sigma)$ of the stresses, $g_D(\omega) \propto \omega^2$ is the Debye DOS, and $\Delta g_{\mathrm{ind}}(\omega)$ and $\Delta g_{\mathrm{dir}}(\omega)$ are the indirect and direct modifications of the DOS. The indirect contributions are proportional to the imaginary parts of the frequency-dependent moduli [28] according to

$$\begin{aligned} \Delta g_{\mathrm{ind}}(\omega) &\propto \omega \,\mathrm{Im}\{\Delta M_L(\omega) + 2\Delta M_T(\omega)\} \\ &\propto \omega^5 P(\sigma)\Big|_{\omega^2 = \sigma/\zeta}. \end{aligned} \tag{13}$$

As $\Delta g_{\mathrm{ind}}(\omega)$ has a frequency dependence with a rather high power (even higher than that of the Rayleigh ω^4 contribution, expected from fluctuating elastic constants [34]), it is not relevant for the low-temperature specific heat, and we discard it from further discussion.

The direct stress-induced contribution to the density of states is

$$\Delta g_{\mathrm{dir}}(\omega) = N_\eta \left\langle \frac{2\omega}{\pi} \mathrm{Im}\left\{ G_{\ell\ell}(\omega) \right\} \right\rangle_{P(\sigma)}. \tag{14}$$

Because the transverse sound velocity in glasses is usually much smaller than the longitudinal one [37], the term $\alpha = T$ in expression (8) for the self-energy $\Delta_\ell(\omega)$ will be dominant, so that we drop the longitudinal term. We further assume a uniform, average transverse coupling $\gamma = \gamma_T^\ell$, so that we have

$$\Delta_\ell(\omega) = \frac{1}{\zeta\mu} (\gamma \sigma_\ell)^2. \tag{15}$$

The direct contribution of the stress-induced terms then becomes (Appendix B)

$$\Delta g(\omega)_{\mathrm{dir}} = \frac{N_\eta}{N} 2\omega P(\sigma)\Big|_{\omega^2 = f(\sigma)}, \tag{16}$$

where N_η is the number of stress-related defect states, and

$$f(\sigma) = \frac{1}{\zeta}\sigma[1 + \gamma^2 \sigma/\mu]. \tag{17}$$

In order to be specific, we now assume that the glassy material is composed of atoms or molecules, which interact via a pair potential $\phi(|\boldsymbol{r}_i - \boldsymbol{r}_j|) = \phi(r_{ij})$. The absolute values of the fluctuating local stresses are given by [25,28]

$$\sigma_{ij} = \left| \frac{1}{\Omega} r_{ij} \phi'(r_{ij}) \right|. \tag{18}$$

Here Ω is a microscopic volume with the size of the order of an interatomic spacing. Because the potential usually has a minimum at a distance r_0, the small values of the stresses are due to distances r_{ij} near this value. In this vicinity we can write

$$\sigma_{ij}(r_{ij}) = \sigma_1 [r_{ij} - r_0]. \tag{19}$$

In the regime around the minimum, where the stresses are very small, we can therefore estimate the distribution density as

$$\lim_{\sigma_{ij} \to 0} P(\sigma_{ij}) = \frac{1}{\left| \frac{d\sigma_{ij}}{dr_{ij}} \right|} 4\pi\rho r_{ij}^2 g(r_{ij}) = \mathrm{const} \doteq P_1, \tag{20}$$

where $\rho = N/V$ is the density of molecules, N their number, V the sample volume, and $g(r)$ the radial pair distribution function [38]. For such a constant distribution density of small local stresses, the expression (14) leads to (Appendix B)

$$\Delta g_\eta(\omega) = n_\eta \frac{\omega}{\sqrt{1+\left(\frac{\omega}{\omega_0}\right)^2}} \tag{21}$$

with $n_\eta = 2N_\eta P_1 \zeta/N$ and

$$\omega_0^2 = \frac{1}{4\zeta\gamma^2}\mu = \frac{1}{\langle r_\perp^2\rangle\gamma^2}\, v_T^2, \tag{22}$$

where we inserted relation (5) for the inertia density. We may introduce the Debye frequency $\omega_D = k_D v_D$ [39] with the Debye velocity

$$v_D^{-3} = \frac{1}{3}(v_L^{-3} + 2v_T^{-3}) \approx \frac{2}{3} v_T^{-3} \tag{23}$$

and the Debye wave number $k_D = (1/a)\sqrt[3]{6\pi^2}$ with the typical distance between molecules $a = \sqrt[3]{m/\rho_m}$, where m is the mass of a molecule (see Ref. [37] for values of k_D of a large number of glasses). Then we can write for ω_0

$$\omega_0 = \frac{1}{\sqrt[3]{9\pi^2}} \frac{a}{\gamma\sqrt{\langle r_\perp^2\rangle}}\omega_D \approx 0.2\frac{a}{\gamma\sqrt{\langle r_\perp^2\rangle}}\omega_D. \tag{24}$$

The frequency regime we are interested in here is the range $\omega \approx 10^{-2}\omega_D$. So, if the ratio ω/ω_0 be of the order of 1, the quantity $\sqrt{\langle r_\perp^2\rangle}\gamma/a$ becomes of the order of 500. This is a reasonable number if we recall that this quantity, which determines ω_0, is the extent of the defects in units of the intermolecular distance times the coupling γ.

Equation (21), together with the definitions in Eqs. (22)–(24), represents the main result of the present Letter, as it gives a quantitative expression for the excess of the DOS at low frequency in glasses.

Before we discuss the implications of our findings for the specific heat, we address the vibrational spectrum of glasses, and in particular the question, why a low-frequency DOS, which varies almost linearly with frequency, has never been reported in the literature. As a matter of fact, both, simulational and experimental determinations of the low-frequency harmonic DOS encounter severe problems. In molecular-dynamics simulations the low-frequency eigenvalues are dominated by the presence of spurious standing waves due to the application of periodic boundary conditions. In order to detect "nonphononic" vibrational excitations, extremely small samples have been investigated, in which the standing waves are suppressed [40–42]. However, as mentioned earlier, it turned out [28] that the low-frequency DOS of such small samples are—via the local stresses—very sensitive to the smoothing ("tapering") of the potential near the imposed cutoff, leading (possibly) to artifacts. In simulations with larger samples $N \sim 10^6$ to 10^7 [43,44] a Debye ω^2 spectrum below the boson peak is observed. As we expect our predicted subquadratic DOS contribution to be very small compared to the Debye law, and the low-frequency data in these simulations exhibit some scatter, we think they are not in conflict with our model.

On the other hand, the experimental determination of the low-frequency vibrational DOS of harmonic excitations suffers from the presence of the anharmonic interactions, which is known to dominate the low-frequency DOS as exhibited by incoherent inelastic scattering data of glasses [45,46]. Coherent inelastic neutron- x-ray, and Raman scattering data do not directly monitor the DOS [47,48], and the low-frequency part in the GHz regime is, again, obscured by anharmonic excitations [49–51]. In order to reveal the low-frequency linear behavior of the vibrational DOS, one would have to do incoherent scattering experiments at very low frequencies *and* very low temperatures, in order to avoid the anharmonic contributions.

At frequencies near one-tenth of the Debye frequency, the mean-free paths of the waves in glasses approach the Ioffe-Regel limit, i.e. its value becomes comparable to their wavelength. In this frequency regime, a peak in the DOS divided by ω^2 is observed, called the boson peak. This anomaly, which shows up in the specific heat as a peak in the quantity $C(T)/T^3$, led to a huge number of experimental and numerical investigations of the vibrational spectrum of glasses [52]. In Refs. [33,36] spatially fluctuating elastic moduli have been identified as the main reason for the boson-peak anomaly. Other authors [17,18] advocated defectlike states, due to soft anharmonic potentials as reason for the anomalies. Such "quasilocalized" excitations [53] are discussed frequently in the recent literature on vibrations in glasses [54,55]. We believe that the stress-related defects states, discussed in Ref. [28] and in the present Letter, are also relevant in the boson-peak spectral regime, in particular the indirect contribution of Eq. (13). This should be the subject of further investigations.

Now we focus on the specific heat that can be calculated from the DOS as [39]

$$C_V(T) \sim \int_0^\infty d\omega g(\omega)(\beta\omega)^2 \frac{e^{\beta\omega}}{[e^{\beta\omega}-1]^2} \tag{25}$$

with $\beta = \hbar/k_B T$.

In order to perform realistic calculations we restore the Debye DOS

$$g_D(\omega) = \frac{3}{\omega_D^3}\omega^2\theta(\omega_D - \omega) \tag{26}$$

where $\theta(x)$ is the Heaviside step function. We then write the relevant DOS as [56]

$$\begin{aligned} g(\omega) &= g_D(\omega) + \Delta g_\eta(\omega) \\ &= \frac{3}{\omega_D^3}\omega^2\theta(\omega_D-\omega) + n_\eta\left(\frac{\omega}{\sqrt{1+\left(\frac{\omega}{\omega_0}\right)^2}}\right). \end{aligned} \tag{27}$$

The specific heat can be now calculated numerically by Eq. (25), using (27). Because the DOS asymptotically

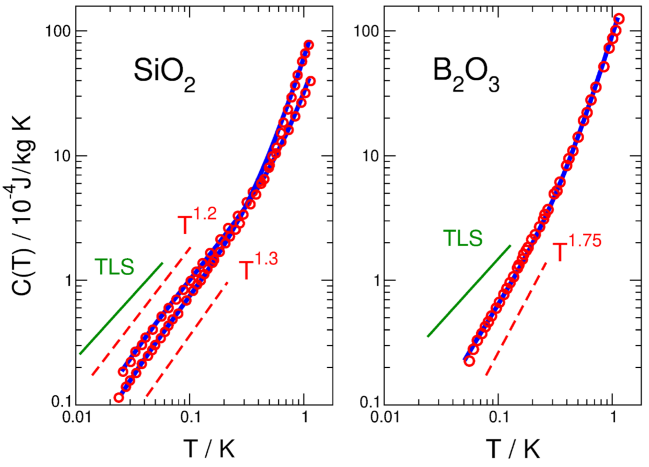

FIG. 1. Left: specific heat of SiO_2 measured by Lasjaunias *et al.* [5] together with fits according to Eqs. (25) and (27) (blue lines). The dataset with apparent temperature dependence $C(T) \sim T^{-1.2}$ is Suprasil with ≈1% OH content, the data with $C(T) \sim T^{-1.3}$ is Suprasil W with only 1 ppm OH. The fit parameters for Suprasil are $\omega_0 = 4.5 \times 10^{-3}$ ps^{-1}, $n_\eta = 5.76 \times 10^{-4}$ ps^2, for Suprasil W $\omega_0 = 6.25 \times 10^{-3}$ ps^{-1}, $n_\eta = 1.28 \times 10^{-4}$ ps^2. Right: specific heat of B_2O_3, measured by Lasjaunias *et al.* [4] (symbols) and calculated via Eqs. (25) and (27) (full blue line). We used the parameters $\omega_0 = 1.5 \times 10^{-2}$ ps^{-1}, $n_\eta = 3.2 \times 10^{-4}$ ps^2. The green lines labeled "TLS" indicate a linearly varying specific heat, which is predicted by the two-level-system tunneling model. The dashed red lines indicate the apparent slopes reported in the original papers [4,5]. For the Debye frequencies we use the values $\Theta_D = 342$ K $\Rightarrow \omega_D = (k_B/\hbar)\Theta_D = 44$ ps^{-1} (SiO_2), $\Theta_D = 153$ K $\Rightarrow \omega_D = 20$ ps^{-1} (B_2O_3) [58].

becomes linear for $\omega \to 0$ we predict $C(T) \propto T^2$ for very low temperatures. If T becomes comparable with $T_0 = \hbar\omega_0/k_B$ a smoothing toward a linear behavior is expected. Finally, depending on n_η, at higher temperature, Debye's T^3 is approached [57].

In Fig. 1 we show the low-temperature specific heat of borate and silica glass as measured some time ago by Lasjaunias *et al.* [4,5]. All datasets do not show a linear but a superlinear temperature dependence, which is obviously well accounted for by our model. We indicated by a green full line the linear law $C(T) \sim T$ corresponding to the prediction of the TLS model in the figure.

The values of ω_0 obtained in the fits for SiO_2 correspond to temperatures $\hbar\omega_0/k_B \approx 40$ mK. For B_2O_3 we get $\hbar\omega_0/k_B \approx 800$ mK. Therefore, we expect that the $C(T)$ of SiO_2 will bend down to show a T^2 law in the T range below 50 mK. $C(T)$ for B_2O_3 extends already to $\hbar\omega_0/k_B$ and will also slightly bend down toward $C(T) \sim T^2$.

Using Eq. (24), we may evaluate the parameter $\sqrt{\langle r_\perp^2 \rangle}\gamma$, the extent of the defects times the coupling for SiO_2 and B_2O_3 from the values of ω_0 obtained by fitting the specific heat. Using the values of the Debye temperature of these materials [58] $\Theta_D = 342$ K (SiO_2), $\Theta_D = 153$ K (B_2O_3), we get, according to Eq. (24) $\sqrt{\langle r_\perp^2 \rangle}\gamma/a \sim 2000$ for Suprasil, $\sqrt{\langle r_\perp^2 \rangle}\gamma/a \sim 1440$ for Suprasil W, and $\sqrt{\langle r_\perp^2 \rangle}\gamma/a \sim 50$ for B_2O_3. The much smaller value of this parameter in B_2O_3 may be rationalized, taking into account that in this material, as opposed to SiO_2, there is a tendency for the formation of layered structural motifs (boxol rings, [59]), which might lead to defect states involving fewer molecular units.

For the low-temperature specific heat we envisage the following scenario: The boson-peak anomaly is in most materials located at one-tenth of the Debye temperature $\Theta_D = \hbar\omega_D/k_B$. Below the boson peak, the quantity $C(T)/T^3$ usually levels off and then begins to rise with decreasing temperature, indicating the cross-over toward the low-temperature regime we are talking about [3,20] The specific heat in glasses is usually measured down to $\approx 10^{-2}\Theta_D$. According to our findings, the temperature dependence in this regime is related to the amount and spatial extension of frozen-in stresses in glasses.

It is important to underline that our model can be tested against future experiments; indeed its prediction implies that $C(T)$ at lower temperatures (around 1 mk) should bend down toward a T^2 law.

It is also interesting to study the development of the low-temperature specific heat as a function of thermal, chemical, or pressure treating. A corresponding change in the prefactor and the crossover parameter ω_0 will give information on the salient features of the internal stresses. This information on the internal stresses will add to the existing disorder classification of glasses, provided by heterogeneous-elasticity theory [33–35,37]. In fact, in a recent study of ultrastable glasses [60] it has been demonstrated that the low-temperature non-Debye specific heat, which was present in the conventional glasses and attributed to tunneling systems, was absent in the ultrastable glasses. Within our new interpretation this means that the frozen-in stresses are strongly reduced in the ultrastable glasses.

Let us finally mention that, of course, the contribution of fluctuating elastic constants, which give rise to Rayleigh scattering and the boson peak [33–35], are not included in the present Letter, which focuses on the frequency regime much below the boson peak. A combined theory (generalized heterogeneous-elasticity theory) for the DOS has been formulated recently [28], and we shall apply it to the specific heat (in comparison with experimental data) in a forthcoming paper.

Data availability—The experimental data in Fig. 1 are taken from Refs. [4,5]. The theory curves in Fig. 1 are obtained analytically by means of Eqs. (25) and (27) using the parameters specified in the text.

[1] R. C. Zeller and R. O. Pohl, Thermal conductivity and specific heat of noncrystalline solids, Phys. Rev. B **4**, 2029 (1971).

[2] W. A. Phillips, *Amorphous Solids: Low-Temperature Properties* (Springer-Verlag, Berlin, 1981).

[3] M. A. Ramos, *Low-Temperature Thermal and Vibrational Properties of Disoredered Solids* (World Scientific, New Jersey, 2022).

[4] J. C. Lasjaunias, D. Thoulouze, and F. Pernot, Non-linear temperature dependence of the low temperature specific heat of vitreous B_2O_3, Solid State Commun. **14**, 957 (1974).

[5] J. C. Lasjaunias, A. Ravex, M. Vandorpe, and S. Hunklinger, The density of states in vitreous silica: Specific heat and thermal conductivity down to 25 mK, Solid State Commun. **17**, 1045 (1975).

[6] R. B. Stephens, Intrinsic low-temperature thermal properties of glasses, Phys. Rev. B **13**, 852 (1976).

[7] R. O. Pohl, Low temperature specific heat of glasses, in *Amorphous Solids, Low-Temperature Properties*, edited by W. A. Phillips (Springer, Heidelberg, 1981), Chap. 3, p. 27.

[8] X. Liu and H. v. Löhneysen, Low-temperature thermal properties of amorphous As_xSe_{1-x}, Phys. Rev. B **48**, 13486 (1993).

[9] P. W. Anderson, B. Halperin, and C. M. Varma, Anomalous low-temperature thermal properties of glasses and spin glasses, Philos. Mag. **25**, 1 (1972).

[10] W. A. Phillips, Tunneling states in amorphous solids, J. Low Temp. Phys. **7**, 351 (1972).

[11] A. Würger, *From Coherent Tunneling to Relaxation*, Springer Tracts in Modern Physics, Vol. 135 (Springer, Heidelberg, 1997).

[12] M. I. Klinger, Soft atomic motion in glasses: Their role in anomalous properties, Phys. Rep. **492**, 111 (2010).

[13] C. C. Yu and A. J. Leggett, Low temperature properties of amorphous solids: Through a glass darkly, Comments Condens. Matter Phys. **14**, 231 (1988).

[14] T. Vegge, J. P. Sethna, S.-A. Cheong, K. W. Jacobsen, C. R. Myers, and D. C. Ralph, Calculation of quantum tunneling for a spatially extended defect: The dislocation kink in copper has a low effective mass, Phys. Rev. Lett. **86**, 1546 (2001).

[15] V. Lubchenko and P. G. Wolynes, Intrinsic quantum excitations of low temperature glasses, Phys. Rev. Lett. **87**, 195901 (2001).

[16] E. R. Grannan, M. Randeria, and J. P. Sethna, Low-temperature properties of a model glass, Phys. Rev. B **41**, 7784 (1990); **41**, 7799 (1990).

[17] V. G. Karpov, M. I. Klinger, and F. N. Ignat'ev, Theory of the low-temperature anomalies in the thermal properties of amorphous structures, Zh. Eksp. Teor. Fiz. **84**, 760 (1983) [Sov. Phys. JETP **57**, 439 (1983)].

[18] U. Buchenau, Y. M. Galperin, V. L. Gurevich, and H. R. Schober, Anharmonic potentials and vibrational localization in glasses, Phys. Rev. B **43**, 5039 (1991).

[19] V. L. Gurevich, D. A. Parshin, and H. R. Schober, Anharmonicity, vibrational instability, and the boson peak in glasses, Phys. Rev. B **67**, 094203 (2003).

[20] M. A. Ramos, Are, "universal" anomalous properties of glasses at low temperatures truly universal?, Low Temp. Phys. **46**, 104 (2020).

[21] U. Fotheringham, Structural and stress relaxation in glass-forming liquids, in *Encyclopedia of Glass Science, Technology, History, and Culture*, Vol. 1, edited by P. Richet (Wiley, Hoboken, NJ, 2021), Chap. 3.7, p. 331.

[22] T. Egami, K. Maeda, and V. Vitek, Structural defects in amorphous solids: A computer simulation study, Philos. Mag. A **41**, 883 (1980).

[23] V. Vitek and T. Egami, Atomic level stresses in solids and liquids, Phys. Status Solidi (b) **144**, 145 (1987).

[24] S.-P. Chen, T. Egami, and V. Vitek, Local fluctuations and ordering in liquid and amorphous metals, Phys. Rev. B **37**, 2440 (1988).

[25] J. F. Lutsko, Stress and elastic constants in anisotropic solids: Molecular dynamics techniques, J. Appl. Phys. **64**, 1152 (1988).

[26] J. F. Lutsko, Generalized expressions for the calculation of eiastic constants by computer simulation, J. Appl. Phys. **65**, 2991 (1989).

[27] S. Alexander, Amorphous solids: Their structure, lattice dynamics and elasticity, Phys. Rep. **296**, 65 (1998).

[28] W. Schirmacher, M. Paoluzzi, F. C. Mocanu, D. Khomenko, G. Szamel, F. Zamponi, and G. Ruocco, The nature of non-phononic excitations in disordered systems, Nat. Commun. **15**, 3107 (2024).

[29] H. Wang, H. Bei, Y. F. Gao, Z. P. Lu, and T. G. Nieh, Effect of residual stresses on the hardness of bulk metallic glasses, Acta Mater. **59**, 2858 (2011).

[30] Y. Wu, A. D. Stoica, Y. Ren, D. Ma, Y. F. Gao, and H. Bei, Direct synchrotron x-ray measurements of local strain fields in elastically and plastically bent metallic glasses, Intermetallics **67**, 132 (2015).

[31] S. Alexander, Is the elastic energy of amorphous materials rotationally invariant?, J. Phys. (Paris) **45**, 1939 (1984).

[32] M. Born and H. Huang, *Dynamical Theory of Crystal Lattices* (Oxford University Press, Oxford, 1954).

[33] W. Schirmacher, Thermal conductivity of glassy materials and the "boson peak," Europhys. Lett. **73**, 892 (2006).

[34] W. Schirmacher, G.Ruocco, and T. Scopigno, Acoustic attenuation in glasses and its relation with the Boson Peak, Phys. Rev. Lett. **98**, 025501 (2007).

[35] W. Schirmacher, T. Scopigno, and G. Ruocco, Theory of vibrational anomalies in glasses, J. Non-Cryst. Solids **407**, 133 (2014).

[36] A. Marruzzo, W. Schirmacher, A. Fratalocchi, and G. Ruocco, Heterogeneous shear elasticity of glasses: The origin of the boson peak, Sci. Rep. **3**, 1 (2013).

[37] Z. Pan, O. Benzine, S. Sawamura, R. Limbach, A. Koike, T. D. Bennett, G. Wilde, W. Schirmacher, and L. Wondraczek, Disorder classification of the vibrational spectra of modern glasses, Phys. Rev. B **104**, 134106 (2021).

[38] J.-P. Hansen and I. R. McDonald, *Theory of Simple Liquids* (Academic Press, New York, 1986).

[39] N. W. Ashcroft and D. Mermin, *Solid State Physics* (Harcourt College Publishers, Fort Worth, 1976).

[40] E. Lerner and E. Bouchbinder, Low-energy quasilocalized excitations in structural glasses, J. Chem. Phys. **155**, 200901 (2021).

[41] M. Paoluzzi, L. Angelani, G. Parisi, and G. Ruocco, Relatiion between heterogeneous frozen regions in supercooled liquids and non-debye spectrum in the corresponding glasses, Phys. Rev. Lett. **123**, 155502 (2019).

[42] M. Paoluzzi, L. Angelani, G. Parisi, and G. Ruocco, Probing the debye spectrum in glasses using small system sizes, Phys. Rev. Res. **2**, 043248 (2020).
[43] L. Wang, A. Ninarello, P. Guan, L. Berthier, G. Szamel, and E. Flenner, Low-frequency vibrational modes of stable glasses, Nat. Commun. **10**, 26 (2019).
[44] H. Mizuno and A. Ikeda, Phonon transport and vibrational excitations in amorphous solids, Phys. Rev. E **98**, 062612 (2018).
[45] J. Wuttke, W. Petry, G. Coddens, and F. Fujara, Fast dynamics of glass-forming glycerol, Phys. Rev. E **52**, 4026 (1995).
[46] A. I. Chumakov, I. Sergueev, U. van Bürck, W. Schirmacher, T. Asthalter, R. Ruffer, O. Leupold, and W. Petry, Collective nature of the boson peak and universal transboson dynamics of glasses, Phys. Rev. Lett. **92**, 245508 (2004).
[47] S. N. Taraskin and S. R. Elliott, Connection between the true vibrational density of states and that derived from inelastic neutron scattering, Phys. Rev. B **55**, 117 (1997).
[48] B. Schmid and W. Schirmacher, Raman scattering and the low-frequency vibrational spectrum of glasses, Phys. Rev. Lett. **100**, 137402 (2008).
[49] U. Buchenau, N. Nücker, and A. J. Dianoux, Neutron scattering study of the low-frequency vibrations in vitreous silica, Phys. Rev. Lett. **53**, 2316 (1984).
[50] M. Foret, E. Courtens, R. Vacher, and J.-B. Suck, Scattering investigation of acoustic localization in fused silica, Phys. Rev. Lett. **77**, 3831 (1996).
[51] R. Vacher, E. Courtens, and M. Foret, Anharmonic versus relaxational sound damping in glasses. II. Vitreous silica, Phys. Rev. B **72**, 214205 (2005).
[52] See Ref. [3], in particular the review article of the present authors for the large number of references on the boson-peak related vibrational anomalies of glasses.
[53] B. B. Laird and H. R. Schober, Localized low-frequency vibrational modes in a simple model glass, Phys. Rev. Lett. **66**, 636 (1991).
[54] F. Vogel and M. Fuchs, Vibrational phenomena in glasses at low temperatures captured by field theory of disordered harmonic oscillators, Phys. Rev. Lett. **130**, 236101 (2023).
[55] E. Lerner and E. Bouchbinder, Boson-peak vibrational modes in glasses feature hybridzed phononic and quadilocalized excitations, J. Chem. Phys. **158**, 194503 (2023).
[56] Here we have considered that n_η is of the order of 10^{-4} ps^2, so that the non-Debye term does not contribute much to the DOS in the frequency regime, where the Debye term is large. Therefore the normalization of the DOS should not be affected by the non-Debye term.
[57] We do not consider the boson-peak anomaly, which occurs at higher frequencies and temperatures than are of interest here.
[58] J. J. Freeman and A. C. Anderson, Thermal conductivity of amorphous solids, Phys. Rev. B **34**, 5684 (1986).
[59] C. Gautam, A. K. Yadav, and A. K. Singh, A review on infrared spectroscopy of borate glasses eith effects of different additives, ISRN Ceramics **2012**, 428479 (2012).
[60] M. Moratalla, M. Rodríguez-López, C. Rodríguez-Tinoco, J. Rodríguez-Viejo, R. J. J. Riobóo, and M. A. Ramos, Depletion of two-level systems in highly stable glasses with different molecular ordering, Commun. Phys. **6**, 274 (2023).

End Matter

Appendix A: Calculation of the Green's functions—We start with the coupled equations (3) of the main text. A Fourier transform with respect to space and time gives ($\alpha = L, T$)

$$[-\omega^2 + v_\alpha^2 k^2] u_\alpha(k,\omega) = \frac{1}{\rho_m} \sum_\ell \gamma_\alpha^\ell \sigma_\ell i k e^{i\mathbf{k}\mathbf{r}_\ell} \eta_\ell(k,\omega),$$
$$\left[-\omega^2 + \frac{1}{\zeta}\sigma_\ell\right] e^{i\mathbf{k}\mathbf{r}_\ell} \eta_\ell(k,\omega) = \frac{1}{\zeta} \sum_{\alpha=L,T} \gamma_\alpha^\ell \sigma_\ell i\mathbf{k} \cdot u_\alpha(k,\omega). \quad \text{(A1)}$$

We may eliminate the vortex fields from these coupled equations, which gives the following effective equations for the longitudinal and transverse fields:

$$[-\omega^2 + v_\alpha^2 k^2] u_\alpha(k,\omega) = -\sum_{\alpha'=L,T} \Delta_{\alpha\alpha'}(k,\omega) u_{\alpha'}(k,\omega) \quad \text{(A2)}$$

with

$$\Delta_{\alpha\alpha'}(k,\omega) = \frac{k^2}{\rho_m \zeta} \sum_\ell \gamma_\alpha^\ell \gamma_{\alpha'}^\ell \sigma_\ell^2 G^{(0)}_{\ell\ell}(\omega). \quad \text{(A3)}$$

We see that the coupling between the elastic degrees of freedom and the vortices induces an indirect coupling between the longitudinal and the transverse waves. Disregarding this coupling, we obtain for the diagonal Green's functions

$$G_{\alpha\alpha}(k,\omega) = \frac{1}{-\omega^2 + v_\alpha^2 k^2 + \Delta_{\alpha\alpha}(k,\omega)}. \quad \text{(A4)}$$

We may as well eliminate the wave fields to obtain

$$\left[-\omega^2 + \frac{1}{\zeta}\sigma_\ell\right] \eta_\ell(k,\omega) = -e^{-i\mathbf{k}\mathbf{r}_\ell} \frac{1}{\rho_m \zeta} \sigma_\ell \sum_\alpha \gamma_\alpha^\ell \frac{k^2}{-\omega^2 + k^2 v_\alpha^2} \times \sum_{\ell'} \gamma_\alpha^{\ell'} \sigma_{\ell'} e^{i\mathbf{k}\mathbf{r}_{\ell'}} \eta_{\ell'}(k,\omega). \quad \text{(A5)}$$

If we average over the positions $\mathbf{r}_\ell$ we get

$$\sigma_\ell \sigma_{\ell'} \langle e^{-i\mathbf{k}\mathbf{r}_\ell} e^{i\mathbf{k}\mathbf{r}_{\ell'}} \rangle_{\mathbf{r}_\ell} = \sigma_\ell^2 \delta_{\ell\ell'} \quad \text{(A6)}$$

from which we obtain

$$\left[-\omega^2+\frac{1}{\zeta}\sigma_\ell\right]\eta_\ell(k,\omega)=-\frac{1}{\rho_m\zeta}\sum_\alpha(\sigma_\ell\gamma_\alpha^\ell)^2\frac{k^2}{-\omega^2+k^2v_\alpha^2}\times\eta_\ell(k,\omega). \tag{A7}$$

In the low-frequency limit this becomes

$$\left[-\omega^2+\frac{1}{\zeta}\sigma_\ell\right]\eta_\ell(k,\omega)=-\Delta_\ell(\omega)\eta_\ell(k,\omega) \tag{A8}$$

with

$$\Delta_\ell(\omega)=\frac{\sigma_\ell^2}{\rho_m\zeta}\sum_\alpha\left(\frac{\gamma_\alpha^\ell}{v_\alpha}\right)^2. \tag{A9}$$

The local Green's function of the vortices is then obtained as

$$G_{\ell\ell}(\omega)=\frac{1}{-\omega^2+\frac{1}{\zeta}\sigma_\ell+\Delta_\ell(\omega)}. \tag{A10}$$

Appendix B: Detailed derivation of the density of states—From Eq. (14) we have

$$\Delta g_\eta(\omega)=N_\eta P_1\frac{2\omega}{\pi}\int_0^{\sigma_{\max}}\omega\delta[\omega^2-f(\sigma)]d\sigma; \tag{B1}$$

with the substitution $\lambda=\omega^2$ we get the level density

$$\Delta\rho_\eta(\lambda)=\frac{1}{2\omega}g\left(\omega=\sqrt{\lambda}\right)=N_\eta P_1\frac{1}{\pi}\int_0^{\sigma_{\max}}\delta[\lambda-f(\sigma)]d\sigma. \tag{B2}$$

We have restricted the integration range in (B2) to positive values of σ. Negative values would lead to negative values of $\lambda=\omega^2$, which is inhibited by the stability requirement for the spectrum. We now further substitute

$$f(\sigma)=\frac{1}{\zeta}\left(\sigma+\frac{\gamma^2}{\mu}\sigma^2\right) \tag{B3}$$

from which follows

$$df=d\sigma\frac{1}{\zeta}\left(1+\frac{2\gamma^2}{\mu}\sigma\right)=d\sigma\frac{1}{\zeta}\sqrt{1+\frac{4}{\mu}\gamma^2\zeta\lambda}, \tag{B4}$$

where the second equality follows from the solution of the equation $\lambda=f(\sigma)$ for σ. We obtain

$$\Delta\rho_\eta(\lambda)=N_\eta P_1\frac{\zeta}{\pi}\frac{1}{\sqrt{1+\frac{4}{\mu}\gamma^2\zeta\lambda}} \tag{B5}$$

from which follows

$$\Delta g_\eta(\omega)=N_\eta P_1\frac{\zeta}{\pi}\frac{2\omega}{\sqrt{1+\frac{4}{\mu}\gamma^2\zeta\omega^2}}. \tag{B6}$$